65° CONGRESSO ABM INTERNACIONAL
65th ABM INTERNATIONAL CONGRESS
ANAIS PROCEEDINGS
ISSN 1516-392X

AN INVESTIGATION ON FRICTION SPOT WELDING IN AA6181-T4 ALLOY[1]

Bruno Parra[2]
Vinícius Toledo Saccon[2]
Nelson Guedes de Alcântara[2]
Tonilson Rosendo[3]
Jorge Fernandes dos Santos[4]

Abstract
Friction spot welding is a new solid state welding process, invented and patented by the GKSS Research Centre GmbH in Germany, suitable for spot joining lightweight low melting point materials such as Al and Mg alloys. The process is performed with an especially designed rotating tool (comprised by a clamping ring, sleeve, and pin) that creates a joint between sheets in overlap configuration by means of frictional heat and mechanical work. The result is a spot welded lap joint with minimal material loss and a flat surface with no keyhole. In this work the application of Friction Spot Welding for spot joining the Al alloy 6181-T4 was investigated. Different rotational speeds (1900 to 2900 rpm) and welding times (2 to 3.4 s) were tested with the objective of finding the best suited ones for producing high quality joints in terms of microstructure and mechanical performance. The mechanical behavior of the joints was investigated by means of shear tensile tests and the final microstructure was assessed using OM and micro hardness measurements. Welds with strength in the order of 6.8 kN were obtained with high reproducibility. The results also showed that geometric elements of the weld play an important role on the fracture mechanisms and hence on the mechanical performance of the joints. In sum, the results revealed the potential of this process for industrial applications.
Keywords: Joining; Welding; Friction spot welding; Aluminum alloy.

INVESTIGAÇÃO DO PROCESSO DE SOLDAGEM POR FRICÇÃO POR PONTO PARA A LIGA AA6181-T4

Resumo
Friction Spot Welding (FSpW) é um processo de solda ponto no estado sólido recentemente desenvolvido no Centro de Pesquisas alemão GKSS. Este processo tem mostrado grande potencial de aplicação frente aos já estabelecidos RSW (automotivo) e rebitagem (aeronáutico). Neste trabalho pretende-se estudar a aplicabilidade deste novo processo para a produção de juntas sobrepostas da liga Al 6181-T4. Esta é uma liga Al-Si-Mg, endurecida por precipitação, que já tem utilização implementada na indústria automobilística. As amostras soldadas foram submetidas a diferentes ensaios mecânicos, além de medições de microdureza para investigação do desempenho mecânico da solda. Análises micro-estruturais utilizando microscopia óptica também foram realizadas, a fim de determinar o efeito dos parâmetros de solda na qualidade micro-estrutural da solda, tão quanto em eventuais defeitos e um estudo de análise de falha visando o entendimento dos mecanismos de fratura, correlacionando-os com os parâmetros de processo.
Palavras-chave: União por fricção; Alumínio; Soldagem.

[1] *Technical contribution to 65th ABM Annual Congress, July, 26th to 30h, 2010, Rio de Janeiro, RJ, Brazil.*
[2] *DEMA – UFSCAR, Rod. Washington Luís – km 235, 13565-905, São Carlos-SP, Brazil. Email: brunoparra@gmail.com*
[3] *PPGEM – UFRGS, Av. Osvaldo Aranha, 99/610, 90035-190, Porto Alegre-RS, Brazil*
[4] *GKSS Research Centre, Institute of Materials Research / Materials Mechanics / Solid State Joining Processes, Geesthacht, Germany*

1 INTRODUCTION

Nowadays, as it has been presented by Pan et al.,[1] spot joints in structural components are achieved mainly by mechanical fastening (clinching, riveting, self-piercing, riveting) and fusion based techniques such as resistance spot welding (RSW) and laser spot welding. Mechanical fastening suffers from a weight penalty, difficulty of automation, requirement for sealants, and corrosion issues. Fusion based spot welding has problems associated to material melting and low weldability issues presented by some high strength lightweight alloys. According to Pan et al.,[1,2] RSW has high costs associated to it due to the large electric supply necessary for lightweight alloys. Sakano et al.[3] and Okamoto[4] also report on these issues adding the decrease of surface quality due to reduced electrode tip life and distortions related to the thermal input causing injuries to the welded parts. Moreover, these fusion techniques usually require chemical cleaning processes of the surfaces prior to welding what may difficult the application to some structures as well lead to environmental problems.

Taking this scenario into account, a relatively new technology, the friction spot welding (FSpW), comes as an alternative to overcome these issues, being capable of replacing those conventional technologies in some applications. FSpW, sometimes referred to as “refill spot welding” or “refill friction stir spot welding”, is a solid-state welding process that produces spot connections suitable for joining parts in overlap configuration. The appearance of the final weld resembles that of a resistance spot welding (RSW), i.e., the surface of the joints is likely to be flat without defects. This process was invented and patented by the GKSS Research Centre in Germany, as reported by Schilling and Santos.[5,6] The absence of keyhole characterizes the FSpW joints as being almost defect free with enhanced mechanical strength. Some other advantages of the process are: environment friendly (no fumes are generated), no additional material is required (ease of recycling), minimal or no waste products, energy efficient, no pre-cleaning necessary as well as no post processing due to good surface quality, fast processing speeds, and ease of automation.

As previously reported by Rosendo et al.,[7,8] sound welds can be obtained with good mechanical behavior and reproducibility by this process, provided that appropriate process parameters and tool configuration are employed. Finally, the mechanical nature of this welding process makes it applicable to any alloy which presents some degree of plasticity, as explained by Schilling et al.,[9] thus low weldability alloys do not represent a concern, and dissimilar joints can also be produced.

The FSpW is performed using a tool assembly comprised of three parts: clamping ring, sleeve, and pin. The Pin and sleeve are operated by separate actuators in such a way that they can be moved up and down independently. The clamping prior to welding is performed by means of a third actuator moving the entire welding head against the work pieces. The clamping ring has two functions: a) to keep the sheets to be welded held tightly during the process and b) work as a barrier to avoid plasticized material to be lost in the form of flash. Both pin and sleeve are connected to one motor (responsible for their rotational speed) and to independent actuators (responsible for the axial displacement).

Depending on which part of the tool is the plunging element, the process can be divided into two variants: pin plunge (FSpW/pin plunge) and sleeve plunge (FSpW/sleeve plunge). In both variants, the process is performed in four stages (see Figure 1). On stage one, the sheets are clamped together by the clamping ring

against a backing anvil and both pin and sleeve start to rotate producing frictional heat on the upper sheet surface (Figure 1a). On stage two, the sleeve is plunged into the sheets while the pin moves upwards creating a cylindrical cavity to accommodate the plasticized material displaced by the sleeve (Figure 1b). After a predetermined plunge depth is reached, the process is reversed marking the third stage where both pin and sleeve retract back to the surface of the upper sheet. The retraction of the pin brings the plasticized material initially displaced back to the hole left by the sleeve, refilling it completely (Figure 1c). Stage four is marked by the withdrawal of the entire welding head from the work pieces, and the result is a flat surface with minimum material loss.

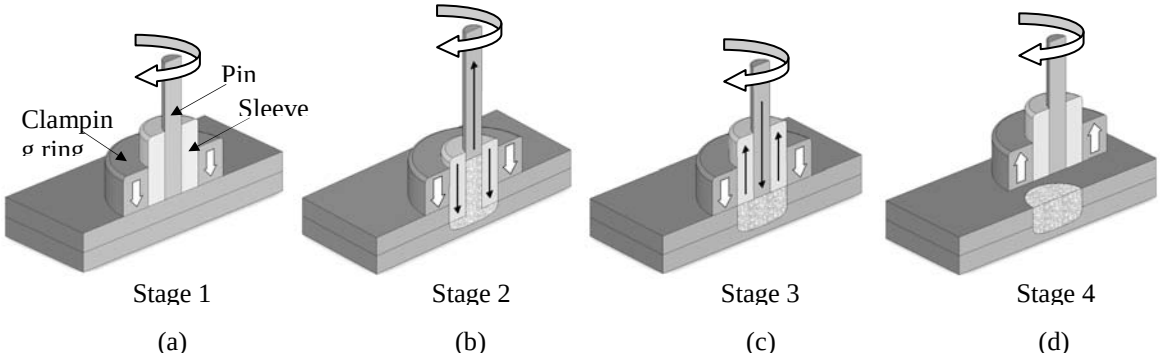

Figure 1. Schematic representation of the FSpW/sleeve plunge process: (a) clamping and spindles rotation, (b) sleeve plunges into the sheets while pin moves upwards, (c) spindles retract back, and (d) withdrawal of welding head.

In this work, the FSpW/sleeve plunge process was used with the objective of investigating the effects of different welding parameters on the microstructural features and mechanical performance of the Al alloy 6181 in the T4 condition. This alloy has strong application in the automotive industry due to its good heat treating properties end ease of recycling. According to Hofmann,[10] these two reasons led to the trend to use only alloys of the 6xxx-series in the automotive structures (unialloy concept). It is worth noting that this work is part of a long term project being developed in the GKSS Research Centre.

2 MATERIALS AND METHODS

Rolled sheets 1.7 mm thick of AA6181-T4 were used to produce overlap joints using the FSpW/sleeve plunge process. The welds were performed using an FSpW prototype machine capable of applying forces up to 15 kN (vertical axis) and reaching a maximum rotational speed of 3000 rpm. A monitoring system recorded the rotational speed, torque, axial load, welding time as well as pin and sleeve position. The welding tool employed had the following dimensions and features: clamping ring – 18 mm diameter, sleeve – 9 mm diameter (with thread feature) and pin – 5.2 mm (with groove features). Details of the tool geometry are shown in Figure 2.

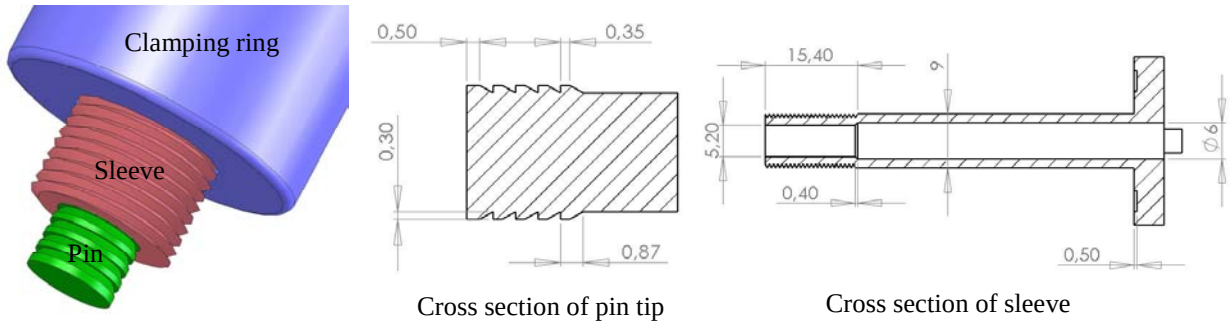

Figure 2. Details of the welding tool used to produce the joint investigated in this work.

A total of 15 different welding conditions (numbered from 1 to 15) were investigated including rotational speed and welding time as process parameter variables. The parameter ranges definition as well as the plunge depth was based on the results of a preliminary investigation performed by Knoll.[11] Table 1 presents the process parameter matrix used to produce the joints investigated.

For each welding condition four overlap joints were produced in the form of samples for shear tensile testing according to the DIN EN ISO 14273 standard.[12] One of the samples was then cut in the centre of the joint for metallographic characterization and hardness evaluation. The other three were submitted to shear tensile testing in order to assess the mechanical resistance of each welding condition. The results obtained with the three samples in the mechanical tests were averaged out for a more reliable indication of the joint strength, and the test reproducibility was evaluated by means of scattering of the results. The shear test samples had a dimension of 230 x 60 mm with 46 mm of overlapping and were tested using a screw-driven testing machine Schenck Trebel RM100 powered by a Zwick controller. The tests were carried out with a displacement rate of 2 mm/min. For the assessment of the weld zones and microstructure of the final joints, the standard metallographic procedure was used to produce samples that were then etched using Kroll solution and electrolytically etched using Barker solution.

Table 1. Welding parameter matrix used to produce the FSpW connections investigated

Process parameters for a sleeve plunge depth of 1.75 mm*															
Welding time [s]	2			2.2			2.6			3			3.4		
Rotational speed [x1000 rpm]	2.9	2.4	1.9	2.9	2.4	1.9	2.9	2.4	1.9	2.9	2.4	1.9	2.9	2.4	1.9
Welding condition	1	2	3	4	5	6	7	8	9	10	11	12	13	14	15

** Taking the upper sheet surface as reference.*

3 RESULTS

Some defects associated to the material flow were found to be present in some joints depending on the welding parameters selected (Figure 3).

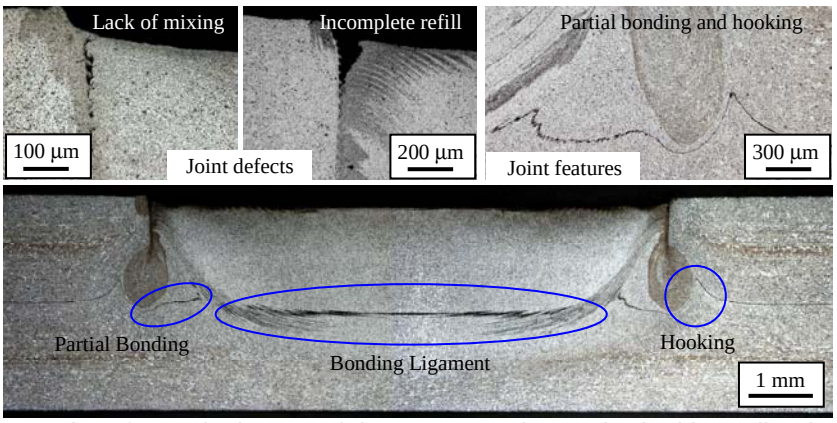

Figure 3. Macrographs of a typical FSpW joint cross section etched with Kroll solution showing the weld zones, joint features, and weld defects.

The micrograph shown in Figure 4a shows the different welding zones, with a detailed image of the SZ in Figure 4b.

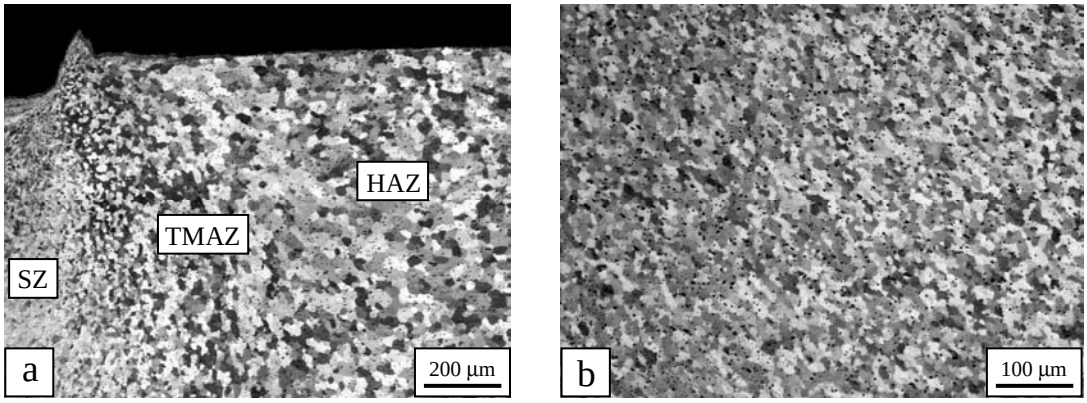

Figure 4. Optical micrographs obtained by electrolytic etching using Barker solution and viewed with polarized light showing details of: (a) distorted grains in the TMAZ and (b) refined microstructure in the SZ.

The Vickers 0.5 microhardness profile is shown in Figure 5, of the cross section of the weld joint.

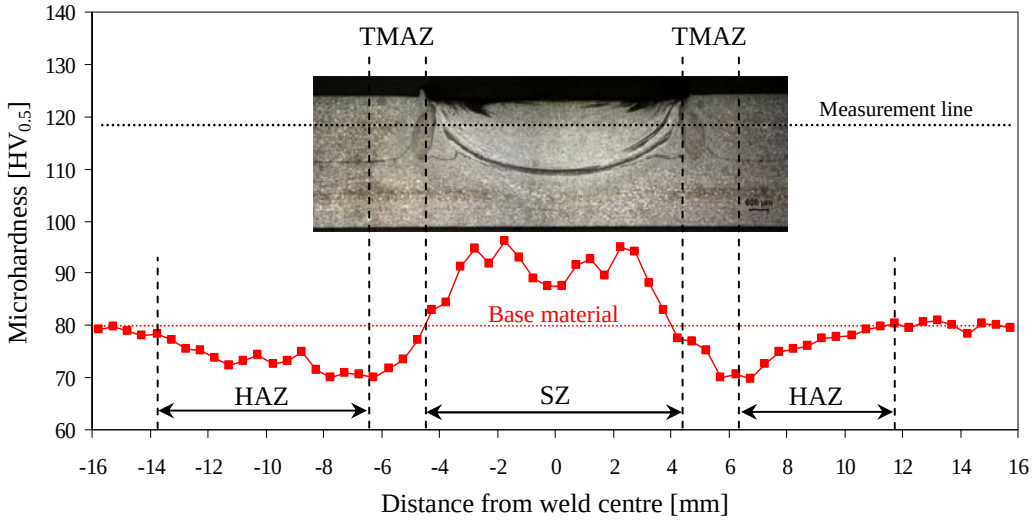

Figure 5. Microhardness profile measured in the middle of the upper sheet at the cross section of a FSpW joint welded according to the welding condition number 10 (2900 rpm / 3 s).

The results of the shear tensile tests, with different welding parameters, are in Figure 6.

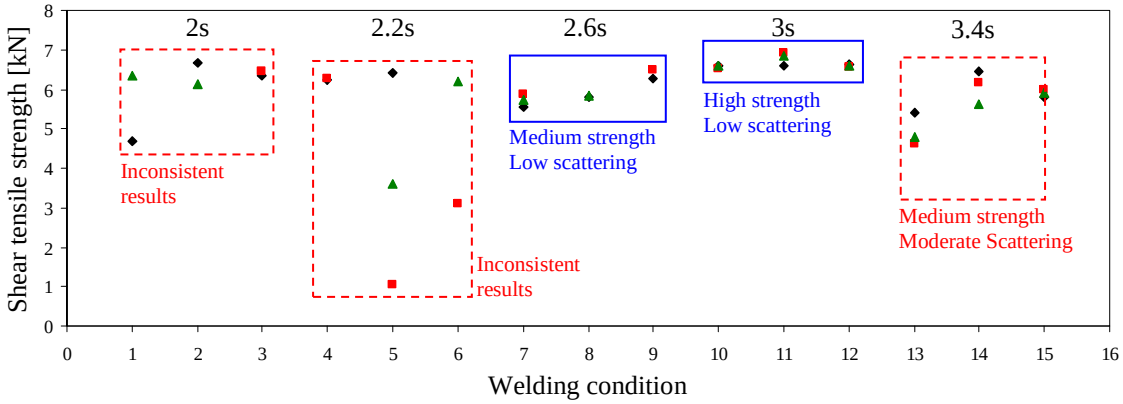

Figure 6. Shear tensile testing results for each welding condition.

The shear tensile resistance of the joints at the optimized welding parameter range (conditions 7 to 12) presented different trends when plotted as a function of the rotational speed, as shown in Figure 7.

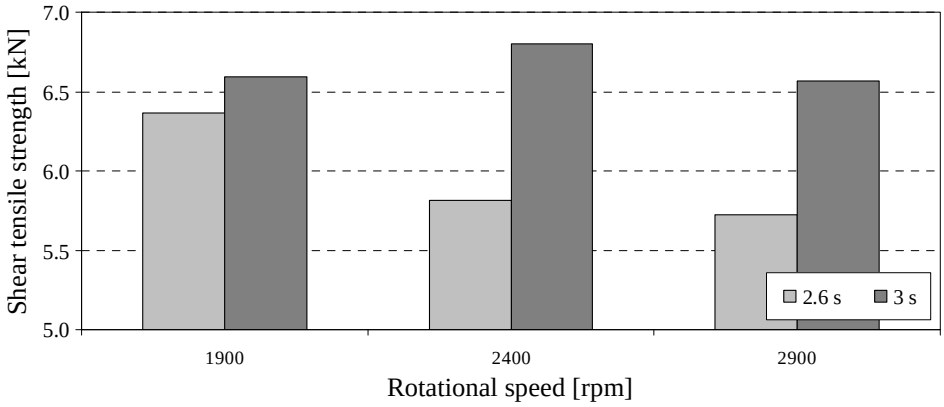

Figure 7. Effect of rotational speed on the joint mechanical strength at the optimized range of welding time.

Analyzing the fractured shear tensile testing samples, three different fracture modes were observed, as shown Figure 8.

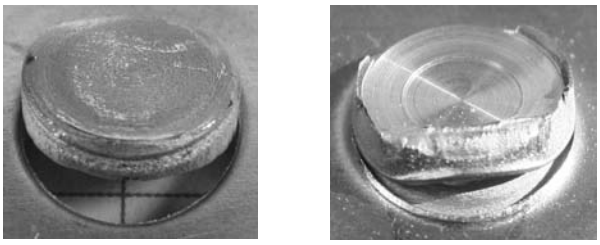

(a) (b)

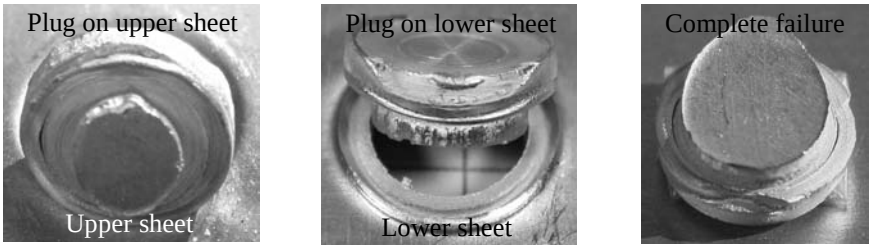

(c)

Figure 8. Fracture modes in shear tensile test: (a) through weld with circumferential crack, (b) plug pull-out with nugget tearing , and (c) plug pull-out with back plug variations.

Schematically showed in Figure 9, the tearing mechanism and the effective shear zone in the crack propagation in shear tensile test.

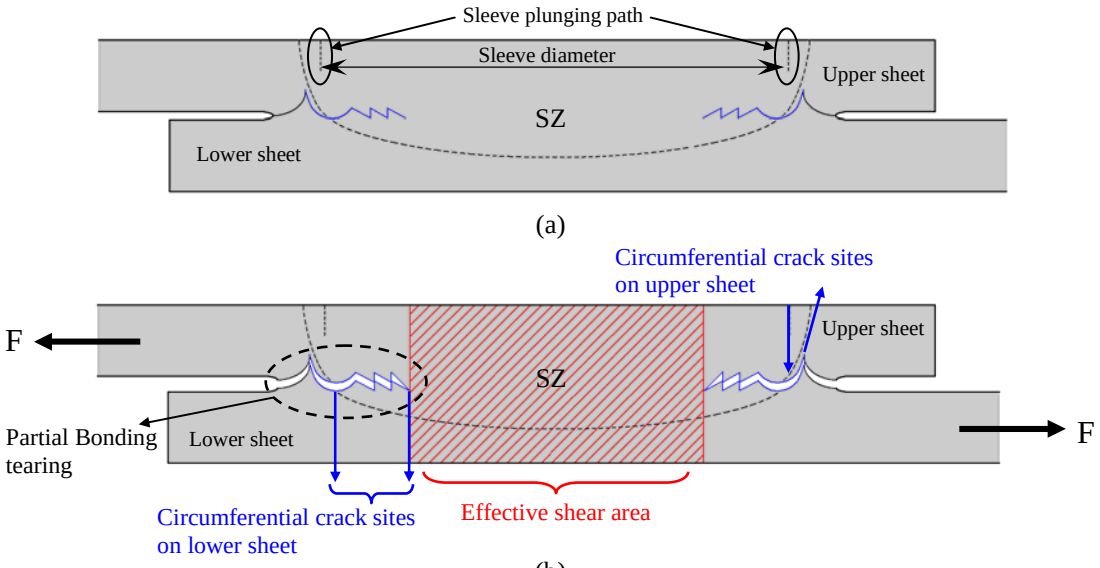

Figure 9. Schematic drawing showing the fracture development of FSpW joints under shear tensile loading. Notice that the joint dimensions are out of proportion for clarity.

The parameters effect in geometry and the mechanical performance of the weld joint are exemplified in Figure 10.

ISSN 1516-392X

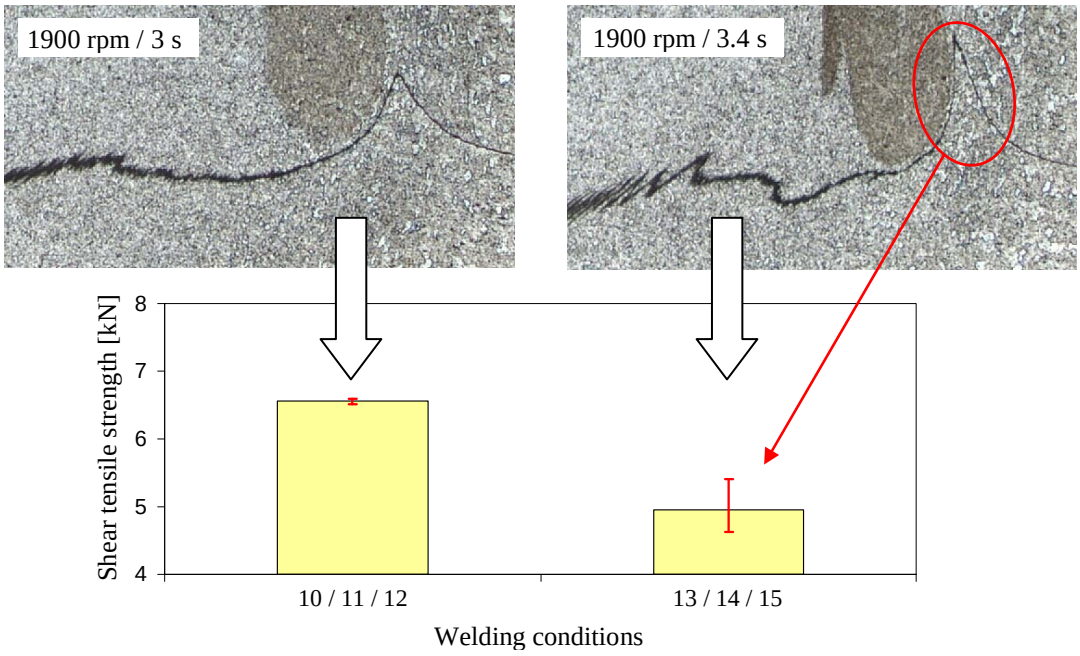

Figure10. Effect of welding time on Hooking sharpness and on joint mechanical performance.

4 DISCUSSION

Optical microscopy (OM) investigation of the welded joints cross section revealed two distinct weld zones: the stir zone (SZ) and the thermo-mechanically affected zone (TMAZ), as shown in Figure 3, similarly to what was described by da Silva et al.[13,14] Nevertheless, a heat affected zone (HAZ) although not resolved with OM is also present, as evidenced by the microhardness profiles across the joint (see Figure 5).

The examination of the cross sections also revealed some geometric patterns common to all the joints, which were referred to as joint elements denominated: Hooking, Partial Bonding, and Bonding Ligament. The Partial Bonding is a kind of transition region where the bonding between the upper and lower sheet is not so strong. It appears as a short and usually uneven line on the joint cross section etched with the Kroll solution and viewed using OM as shown in Figure 3. The Bonding Ligament is a region of good adhesion between the upper and lower sheet with strong resistance. Its characteristic shape on the edges (Figure 3) is a result of the material flow, especially on the third stage of the process, when the pin pushes the plasticized material (displaced on the second stage) back to its original position. The Hooking is caused by the plastic deformation of the lower sheet, and its final dimensions will be controlled by the energy input. It presents an upside down V shaped appearance, as shown in Figure 3.

The defects associated to the material flow (Figure 3) were referred to as lack of mixing and incomplete refill, both located at the path through which the sleeve plunges into the upper sheet. Their occurrence was found to be associated to improper combination of the rotational speed and welding time. The macro- and micrographs of the joint cross section shown in Figure 3 were etched with Kroll solution.

The TMAZ is characterized by grains distorted in comparison to the base material. Moderate strain rate accompanied by moderate temperature are responsible for the microstructural changes in this zone. Higher magnification

micrographs of this weld zone revealed elongated grains pointing upwards at the vicinity of the SZ, see Figure 4a. The exact extension of the TMAZ is not easily measured, but comparisons between the micrographs and hardness profiles show an average extension of 1.6 mm away from the SZ for the welds produced in this work.

The SZ is characterized by very refined and rather equiaxed grains as shown in Figure 4b. This microstructure appearance is associated to dynamic recrystallization caused by the high strain rate during the plunging stage and the thermo cycle imposed by the process, as explained by Gerlich et al.[15] The micrographs shown in Figure 4 were obtained with electrolytic etching using Barker solution and observed with OM using polarized light.

Since the AA6181 is a precipitation hardening alloy, the changes of the precipitates during and after welding will be the most important phenomena dictating the resulting hardness and strength of the different weld zones. The mechanical and thermal inputs provided by the welding tool in friction based welding processes have proven to affect the original state and distribution of the precipitates. Such changes were evidenced by TEM observations of the different weld zones by Olea et al.[16] Nevertheless, the microhardness profile at the cross section of the welded specimens (Figure 5) can also be used to infer these changes. The base material presents an average hardness of 80 $HV_{0.5}$ which starts to decrease in the HAZ to a minimum of 70 $HV_{0.5}$ at the interface between HAZ and TMAZ. The hardness loss at the outer limits of the HAZ is associated mainly to the recovery of the rolled microstructure of the base material since the temperature reached at this site is not so high during welding. However, the closer to the centre of the weld, the higher is the peak temperature reached, and the strengthening particles can be subjected to coarsening and even solubilization. Coarsening has shown to be the predominant phenomenon in the TMAZ due to the thermocycle in this weld zone according to the TEM observations reported by Olea et al.[17] The deformation level can also produce some strain hardening in the TMAZ although not enough to suppress the softening due to precipitate coarsening.

In the SZ, as mentioned above, the intense plastic deformation and high temperatures cause the microstructure to undergo dynamic recrystallization. The high temperature will lead to the solubilization of the precipitates, and their re-precipitation during cooling right after welding is thought to be the main reason for the hardness increase in this zone. Figure 5 also shows that the average hardness in the SZ is higher in comparison to that in the base material which presents a T4 (solution plus natural aging) heat treatment. The authors believe this behavior is probably associated to the fact that in the SZ there are two mechanisms taking place together and favorable to the strengthening of the material: reduction of grain size and re-precipitation accompanied by aging. The T4 heat treatment offers a medium level of strengthening to the alloy which is overcome by the recrystallized and re-precipitated microstructure at the SZ after cooling. Therefore, it is assumed that the temperature reached in the SZ is high and the time the material is exposed to this high temperature is long enough to lead to a substantial level of solubilization which will later lead to re-precipitation.

The shear tensile tests revealed that some sets of welding parameters resulted in high strength joints with reproducibility while others were associated to weak joints and/or scattering. Figure 6 presents the maximum load achieved during shear tensile testing of each welding condition. According to the strength and repeatability presented by the welding conditions in this test, the joints were classified as sound or poor joints.

It can be seen that the best welding conditions were those with total welding time between 2.6 s and 3 s (conditions 7 to 12), that is, welds with slower plunge rates. From these best conditions, parameter sets 10 and 12 presented the lowest scattering with standard deviation of 0.05 and 0.04 respectively. Condition 11 presented a little bit higher scatter (std dev = 0.17) with practically the same average joint resistance (6.8 kN against 6.6 kN of both conditions 10 and 12).

It can be seen in Figure 7 that for the welding time of 2.6 s the joint strength decreases as the rotational speed increases. On the other hand for the welding time of 3 s the average strength is apparently insensitive to the rotational speed.

Based on these results and considering the equation proposed by North et al.,[18] which shows the rotational speed and welding time as the two process parameters that affect mostly the energy input, it can be said that the 3 s welding time provides the amount of energy necessary to produce sound joints for this alloy. When a slightly shorter welding time was employed (2.6 s), the stronger joints were associated to slower rotational speeds. This may be associated to the slip between the rotating sleeve and the surrounding material during welding under faster rotational speeds (accompanied by short welding time) concentrating the energy input at the vicinity of the welding tool.

Based on a standard nomenclature adopted by Koch et al.[19] and Allen et al.,[20] the fracture modes observed in this work were referred to as: a) through weld with circumferential crack (Figure 8a), b) plug pull-out with tearing (Figure 8b), and c) plug pull-out with back plug; this last one presents three variants, see Figure 8c. These fracture modes were observed both in sound and poor joints with the exception of the plug pull-out with back plug variants: plug on upper sheet and plug on lower sheet, see Figure 8c. These two variants were associated to sound and poor joints respectively.

All the fracture modes were associated to the same fracture initiation mechanism. In this fracture initiation stage, the Partial Bonding region plays an important role. When a sample is loaded during the shear tensile test, the two sheets tend to get separated at the Partial Bonding by a tearing mechanism, as schematically indicated in Figure 9. This separation (tearing) leads to the formation of an annular crack surrounding the SZ. Depending on the properties of the other weld zones, this annular crack may grow through the Bonding Ligament. As a consequence of this annular crack, the effective shear area of the joint becomes smaller, see Figure 9b.

Following the Partial Bonding tearing, it was observed that circumferential cracks may nucleate on just one or on both sheets. On the upper sheet, the only two nucleation sites observed were the Hooking tip and the welding defects (lack of mixing and incomplete refill) at the sleeve plunging path, see Figure 9a. On the lower sheet, it usually initiates at two sites as well, one is the tip of the annular crack (formed by the tearing of the Partial Bonding feature) and the other is the interface between the Partial Bonding and the Hooking, see Figure 9a. The overall properties of the joint will determine the subsequent fracture mechanisms that will lead to the final fracture of the joint. An in depth explanation of these fracture mechanisms is not within the scope of the present study and will be published elsewhere.

Since the Hooking works as a crack nucleation site, when it becomes too sharp a crack can nucleate and grow on the upper sheet under small loading levels. The micrographic analysis showed that the Hooking sharpness is strongly related to the welding time. It was observed that the Hooking gets too sharp for welding times longer than 3 s due to the high level of plasticity of the lower sheet caused by the

intense energy input provided by such long welding times. This observation explains the deterioration of the joint mechanical strength when the welding time was increased from 3 s to 3.4 s, as previously shown in Figure 6. Comparing the cross section of joints produced with 3 s and 3.4 s shows, the differences concerning the Hooking geometry (specially its sharpness) can be clearly seen, as shown in Figure 10.

5 CONCLUSIONS

In this study, the applicability of the new Friction Spot Welding process for producing overlap joints of Al alloy 6181-T4 in the T4 condition was investigated. A welding parameter matrix was established based on previous experiences of the group, and the joints produced were characterized in terms of metallurgical and mechanical performance.

The results revealed that sound joints can be produced, and the strongest joints were associated to welding time between 2.6 s and 3 s, especially when accompanied by slow rotational speed (1900 rpm). The joint cross section revealed the joints are formed by three elements: Partial Bonding, Bonding Ligament and Hooking. The combination of the welding time and rotational speed (i.e. energy input) showed strong influence on these elements as well as eventually causing some weld defects (lack of mixing and incomplete refill).

Welding times shorter than 3 s led to high strain rate in the material surrounding the tool (due to the fast plunge rate) causing weld defects. At the optimum welding time range of 2.6 s and 3 s, the rotational speed showed to have little effect on the joint strength indicating that the welding time is the major parameter providing the energy input necessary to produce a proper connection between the upper and lower sheet. Finally, the Hooking geometry plays an important role in the development of the fracture, and it is responsible for the decrease of the strength in the joints produced with welding times longer than 3 s.

Acknowledgments

This work has been carried out as part of a DAAD/CAPES program with additional support of the Technology Transfer Department of the GKSS Research Centre GmbH. Many thanks to Riftec GmbH for producing the joints investigated in this work. The authors would also like to express their appreciation to Mrs. Petra Fischer for her support in the preparation of the metallographic specimens and special thanks to CNPQ for some support to this work.

REFERENCES

1 PAN, T., ZHU, W., SCHWARZ, W., 2005. Spot Friction Welding for aluminium sheets. Proceedings of the 2005 International Automotive Body Congress, September 20-21, vol 2, Ann Arbor, Michigan, USA, pp. 95-99.

2 PAN, T., et al., 2006. A Feasibility Study on Spot Friction Welding of Magnesium Alloy AZ31. Proceedings of the 63rd Annual World Magnesium Conference, May 21-24, Beijing, China.

3 SAKANO, R., et Al., 2001. Development of Spot FSW Robot System for Automobil Body Members. 3rd International Friction Stir Welding Symposium, September 27-28, Port Island, Kobe, Japan.

4 OKAMOTO, K., HUNT, F., HIRANO, S., 2005. Development of Friction Stir Welding Technique and Machine for Aluminum Sheet Metal Assembly. SAE International.
5 SCHILLING, C., DOS SANTOS, J.F., 1999. Verfahren und Vorrichtung zum Verbinden von wenigstens zwei aneinanderliegenden Werkstücken nach der Methode des Reibschweissens. Patent Application Amtl. Az. 199 55737.3.
6 SCHILLING, C., DOS SANTOS, J.F., 2005. Method and Device for Linking at Least Two Adjoining Work Pieces by Friction Welding. International Patent Publication WO/2001/036144.
7 ROSENDO T., et al., 2007. Friction spot welding of AA2024 T3 aluminium alloy a feasibility study, Euromat 2007, September 10th–13th, Nuremberg, Germany.
8 ROSENDO T., et al., 2008. Investigation of friction spot welding of aeronautic AA2024-T3 and AA7075-T6 alloy. 8th International conference on trends in welding research, June 2-6, Pine Mountain, Georgia, USA.
9 SCHILLING, C., STROMBECK, A.V., DOS SANTOS, J.F., 2001. Friction Spot Welding – New Joining Process for Spot Connections. GKSS Research Center Internal Report, Geesthacht, Germany.
10 HOFMANN, A., 2001. Deep drawing of process optimized blanks. Journal of Materials Processing Technology 119, pp. 127-132.
11 KNOLL, H., 2007. Untersuchungen von Reibpunktschweißverbindungen in Aluminiumlegierungen. Bachelor Thesis. Fachhochschule Düsseldorf, University of Applied Sciences, Düsseldorf, Germany.
12 DIN EN ISO 14273, 2002-03. Specimens Dimensions and Procedure for Shear Testing Resistance Spot, Seam and Embossed Projection Welds. International Standard.
13 SILVA, A.M. et al., 2007a. Friction based spot welding processes – Literature Review, Welding and Material Testing, ISSN 1453-0392.
14 SILVA, A.M., et al., 2007b. Preliminary Investigations on Microstructural Features and Mechanical Performance of Friction Spot Welding of Aluminium Alloys. IIW International Seminar on Friction based Spot Welding Processes, GKSS Research Centre. March 29-30, Geesthacht, Germany.
15 GERLICH, A., Su, P., YAMAMOTO, M., NORTH, T., 2007. Effect of welding parameters on the strain rate and microstructure of friction stir spot welded 2024 aluminium alloy. Journal of Material Science.
16 OLEA, C., et al., 2007. A sub-structural analysis of friction stir welded joints in an AA 6056 Al-alloy in T4 and T6 temper conditions. Materials Science and Engineering, A454-455, pp. 52-62.
17 OLEA, C., 2008. Influence of energy input in friction stir welding on structure evolution and mechanical behaviour of precipitation-hardening in aluminium alloys (AA2024-T351, AA6013-T6 and AL-Mg-Sc). PhD Thesis, Mechanical Engineering Department, University of Bochum, Bochum, Germany.
18 NORTH, T., et al., 2005. Understanding friction welding. Proceedings of inter-university research seminar (IURS 200), Beijing, China.
19 KOCH, N., PODRAZA, D., FREEMAN, J., ARBEGAST, W.J., 2003. An Investigation of Friction Spot Welding of Thin Aluminum Sheets. Aeromat 2003, 14th Advanced Aerospace Materials & Processes Conference and Expositions, Dayton, USA.
20 ALLEN, C., ARBEGAST, W.J. 2005. Evaluation of Friction Spot Welds in Aluminum Alloys. Technical paper 2005-01-1252. SAE International.